

**INTERNATIONAL ORGANISATION FOR STANDARDISATION  
ORGANISATION INTERNATIONALE DE NORMALISATION  
ISO/IEC JTC1/SC29/WG11  
CODING OF MOVING PICTURES AND AUDIO**

**ISO/IEC JTC1/SC29/WG11 MPEG2014/M34292  
July 2014, Sapporo, Japan**

**Source** Instituto de Telecomunicações, Portugal  
PEE/COPPE/DEL/Poli, Universidade Federal do Rio de Janeiro, Brazil,  
Poznan University of Technology  
Chair of Multimedia Telecommunications and Microelectronics

**Status** Contribution

**Title** Intra depth-map coding using flexible segmentation, constrained depth modeling modes and simplified/pruned directional prediction

**Author** Luís F. R. Lucas  
Krzysztof Wegner  
Nuno M. M. Rodrigues  
Carla L. Pagliari  
Eduardo A. B. da Silva  
Sérgio M. M. de Faria

## **1 Abstract**

An alternative encoding solution for efficient intra-based depth map compression is proposed. The algorithm, named Predictive Depth Coding (PDC), was specifically developed to efficiently represent the characteristics of depth maps, mostly composed by smooth areas delimited by sharp edges. At its core, PDC involves a sophisticated intra prediction framework and a straightforward residue coding method, combined with an optimised flexible block partitioning scheme. In order to improve the algorithm in the presence of depth edges that cannot be efficiently predicted by the intra directional modes, a constrained depth modelling mode, based on explicit edge representation, was developed.

The performance of the proposed intra depth map coding approach was evaluated based on the quality of the synthesised views using the encoded depth maps and original texture views. The results showed a higher rate-distortion efficiency of the PDC algorithm over the current state-of-the-art depth map coding solution used by the 3D extension of the High Efficiency Video Coding (3D-HEVC) standard. Furthermore, an average reduction of 25% in computational complexity was observed over the 3D-HEVC standard, for depth map coding only.

## **2 Introduction**

3D video coding extension to the HEVC standard, known as 3D-HEVC [1] is currently state of the art technique for efficient 3D video representation in video plus depth data format. Video and depth are coded jointly exploiting each other's redundancy to enhance coding efficiency.

But 3D-HEVC can be also used for depth coding only. Intra-based depth coding technique implemented in 3D-HEVC employs transform coding with directional intra prediction, as typically used for texture image coding. However, in order to represent depth map features better (such as sharp spatial edges), new coding tools, like depth modelling modes, depth lookup table, region

boundary chain code, simplified depth coding and view synthesis optimization were introduced. Furthermore, 3D-HEVC disables all in-loop filters which were designed for natural image coding.

While depth coding used in 3D-HEVC is very sophisticated there is still room for improvements.

Over the years many depth coding techniques have been developed. Previous work on depth map coding using the JPEG-2000 standard, which is based on wavelet transform, has been considered in literature. An improved solution, known as platelet-based algorithm [2], approximates the blocks resulting from a quadtree segmentation of the depth map by using different piecewise-linear modeling functions. Smooth blocks are approximated by using a constant or a linear modeling function. Blocks with depth discontinuities are modeled by a wedgelet function, defined by two piecewise-constant functions, or by a platelet function, defined by two piecewise-linear functions, both separated by a straight line. Despite the provided performance improvements, recent work on depth map coding using a preliminary version of the proposed method has shown to outperform Platelet algorithm.

This document presents an alternative depth coding solution based on intra techniques for efficient compression of depth maps. Unlike 3D-HEVC, the developed algorithm efficiently exploits the capabilities of directional intra prediction using a very flexible block partitioning scheme. Some improvements to intra prediction scheme are also proposed by means of an adaptative reduction of available modes and a new prediction mode based on depth modelling. A preliminary version of this algorithm can be found in [3].

### **3 Algorithm Description**

PDC algorithm uses a block-based hybrid coding approach based on intra prediction and residue coding (see Figure 1). The depth image is partitioned into non-overlapping blocks of 64x64 pixels that can be further partitioned into smaller sub-blocks using a very flexible partitioning scheme (see sec 3.1). Each sub-block can be predicted from a neighbouring block by intra directional prediction or alternatively by new constrained depth modeling modes.

The intra directional prediction is based on the planar, DC and angular modes proposed in HEVC standard [4]. Significant improvement in adaptative direction reduction and signaling has been proposed (see sec 3.2).

The sub-block may alternatively be encoded using a constrained depth modelling mode, designed for explicit signaling the edges that are difficult to predict (see sec 3.3). This kind of edges are typically observed in the bottom-right region of the block, which cannot be predicted by directional intra prediction modes using left and top neighbouring block samples. The proposed constrained depth modelling mode allows to explicitly signal an approximation of the edges in the block and surrounding smooth areas.

PDC doesn't use transform based residual information coding. Instead PDC encodes the residual information, given by the difference between the original and predicted signal, using a straightforward and efficient method that applies linear approximations to the residue signal, depending on the chosen prediction mode.

Like 3D-HEVC, PDC exploits a depth lookup table to efficiently encode the residue signal values, mainly when depth maps present a very restricted depth range.

On the encoder side, most of the possible combinations of block partitioning and coding modes are examined and the best one is selected according to a Lagrangian rate-distortion cost. Context adaptive m-ary arithmetic coding (CAAC) is used for entropy coding.

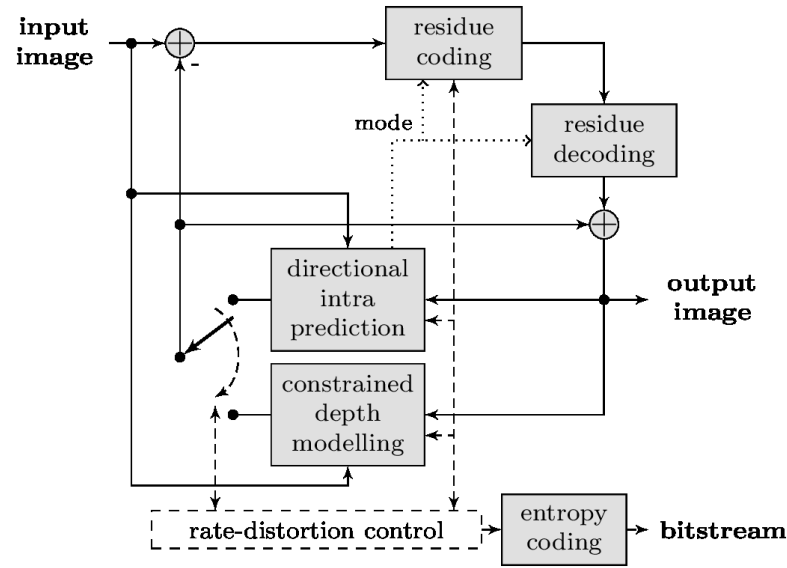


Figure 1: Block diagram of the proposed intra PDC algorithm.

### 3.1 Flexible Block Partitioning

During the encoding process, each block can be partitioned through a flexible scheme which is a combination of bitree and quadtree method. Flexible partitioning scheme recursively divides the block, either in the vertical or horizontal directions, down to the 1x1 size. The used block sizes are illustrated in Figure 2. Note that, block sizes with a high ratio between horizontal and vertical dimensions (ratios larger than 4, e.g. 64x1) are not included in the proposed partitioning scheme because they significantly increase the encoder's computational complexity and have a small impact on the rate-distortion performance.

The quadtree block partitioning was combined with bitree flexible partitioning scheme in order to further reduce the encoder's computational complexity. Three quadtree levels were defined at block sizes 16x16, 32x32 and 64x64. The four partitions, generated by each quadtree partitioning, are processed using a raster scan order.

For each presented quadtree level, the flexible partitioning can be used within a restricted range of block sizes, which depends on the block area. Table 1 presents the proposed maximum and minimum block areas (and block sizes) that are generated by the flexible block partitioning scheme, for each available quadtree level.

Table 1: Flexible segmentation restrictions per quadtree level.

Quadtree level	Max. block area	Min. block area
2	4096 (64x64)	256 (16x16)
1	1024 (32x32)	64 (8x8)
0	256 (16x16)	1 (1x1)

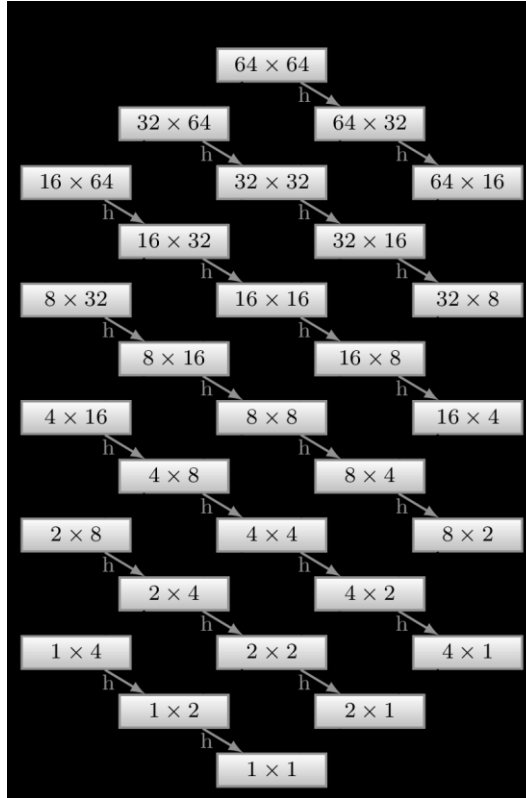


Figure 1: Possible block sizes in PDC and respective label numbers.

### 3.2 Directional Intra Prediction

Combined with the flexible block partitioning scheme, the directional intra prediction framework provides an efficient representation for depth map edges. The proposed intra prediction framework is based on the one proposed to the current state-of-the-art HEVC standard. It includes the intra planar, DC and 33 angular prediction modes [4]. In this algorithm, some improvements and simplifications were made for better prediction of depth map signals.

#### 3.2.1 Pre-defined reduction of directional modes

As previously explained, PDC uses a great amount of block sizes which can be predicted based on 33 directional intra modes. Since some block sizes are very small or narrow, some directional intra prediction modes, namely adjacent directions, may be redundant and produce very similar prediction patterns. For example, the 1x4 block size presents very few samples in the horizontal direction (1-wide width), which is not sufficient to project the left neighbour reference samples into 17 clearly distinct prediction directions (angular 2 up to angular 18 modes).

In this context, in order to avoid unnecessary calculations and to use less bits for directional intra prediction coding, a pre-defined reduction in the set of available prediction directions was proposed for some block sizes.

#### 3.2.2 Adaptive reduction of directional modes

Because depth maps present large smooth areas, multiple prediction directions may produce the same predicted samples. In order to exploit this prediction redundancy, and adaptive reduction of available directional modes is proposed, depending on the reference samples in the neighbouring of each block to be predicted. This method provides both speed-up of the encoder and bitrate reduction, since a more limited set of directions is tested, and fewer bits are required to signal each directional mode.

The proposed method defines three groups of directional prediction modes, which may be disabled as a whole when the associated neighbouring reference samples are exactly constant. These groups of prediction modes and associated neighbouring regions are shown in Table 2. The group 1 contains all the directions that generate a prediction signal exclusively based on the top and left neighbourhood including the top-left pixel. When these reference samples are constant, the associated modes of group 1 are disabled. DC mode can be chosen in place of the disabled modes of group 1, since it produces the same predicted samples. When the samples of the neighbour left and down-left regions are constant, the modes of group 2 can be disabled. In this case, the angular 10 mode (horizontal) is able to substitute these modes, producing the same results. Group 3 contains those modes that depend on top and top-right neighbour regions, and can be replaced by angular mode 26 (vertical).

Table 2: Groups of prediction modes defined according to the block neighbour regions.

Group	Neighbour regions	Prediction modes
1	top & left & top-left	modes 10 to 26, planar
2	left & down-left	modes 2 to 9
3	top & top-right	modes 27 to 34

### 3.3 Constrained Depth Modelling Mode

The main idea behind constrained depth modelling mode (CDMM) is to boost the intra directional prediction, by providing an alternative method that explicitly encodes depth edges in the bottom-right region of the block, that are hard to predict by directional intra prediction. This method is inspired on depth modelling modes used in 3D-HEVC, but several restrictions were applied to its design, in order to make it more efficient in the context of the PDC algorithm.

Intra prediction angular modes are able to represent most of the straight edges present in depth maps. However, some specific ones are difficult to predict. An example of a straight edge that is difficult to predict is illustrated in Figure 3. PDC intra prediction framework reasonably predicts straight edges coming from the left or top block neighbourhood. When an edge does not touch the left or top neighbour samples, like the one shown in the right block of Figure 3, it becomes difficult to predict.

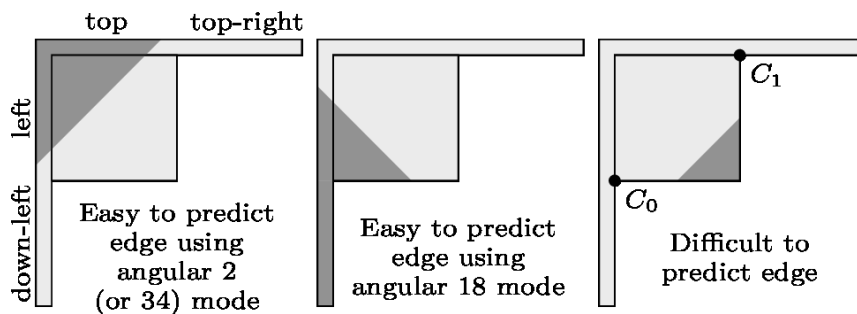


Figure 2: Example of easy to predict edges (left and middle) and difficult to predict edge (right).

The principle of the proposed CDMM consists in dividing the block into two partitions, which are approximated by constant values. The block partitioning should occur between two points of the right and bottom margins of the predicting block. As a second restriction to the proposed method, the line drawn between the two chosen points should be parallel to the diagonal defined by the down-left and top-right block corners. This way, it can be specified by just one parameter.

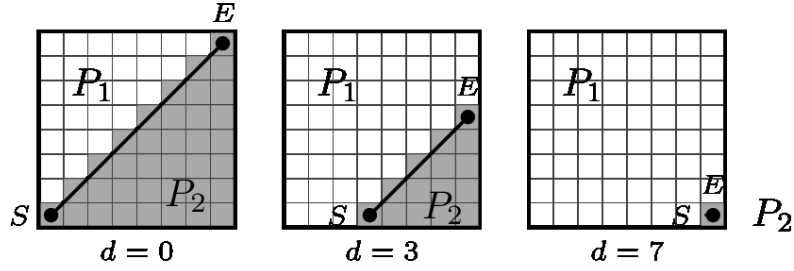


Figure 3: Block partition examples using the proposed constrained depth modelling mode.

Figure 4 illustrates some partition possibilities of the proposed CDMM for an 8x8 square block. The imposed constraints highly simplify the signalling of the CDMM block partition, requiring a single value only, which is represented by the offset  $d$  in Figure 4. In this example, eight different partitions that vary between the minimum offset,  $d=0$ , and the maximum offset,  $d=7$ , can be employed. It can be observed in Figure 4 that block partitions are performed in the bottom-right half of the block and their slope is the same as the block down-to-top diagonal, satisfying the proposed constraints.

The restriction on the block partitioning slope is advantageous in terms of computational complexity because it avoids testing a lot of block partitions with different slopes. Furthermore, by using a unique partition slope associated with the block size, no bitstream overhead is required for its transmission. The main disadvantage of this partitioning restriction is the reduced flexibility to approximate depth map edges. However, the proposed PDC algorithm is able to alleviate this issue, by combining CDMM with the flexible partitioning scheme.

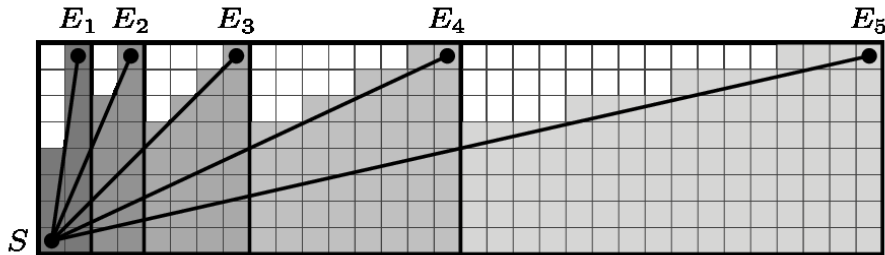


Figure 4: Different CDMM partition slopes provided by flexible partitioning.

The large amount of block sizes generated through flexible partitioning provides up to five different CDMM partitioning slopes according to the possible down-to-top diagonals. Figure 5 illustrates these five CDMM line partition slopes generated from different block sizes available in the PDC algorithm. The blocks are overlapped and the available slopes are represented between the points  $S$  and  $E_n$ , for  $n=1,2,3,4,5$ . The illustrated overlapped block sizes represent all the block width/height ratios available in PDC. CDMM block partitioning generates two partitions, whose depth values are approximated by using a constant value. For  $P_1$  partition, the approximation coefficient is derived from the block neighbourhood, namely through the mean of the left and top neighbouring reconstructed samples. The constant approximation of  $P_2$  partition is explicitly transmitted to the decoder. For that, the mean value of the original samples in  $P_2$  is computed and the difference between the constant values  $P_1$  and  $P_2$  is encoded using the DLT technique. The residual information generated by the proposed approximation is bypassed, not requiring any extra bits.

### 3.4 Residual Signal Coding

The flexible block partitioning scheme combined with the directional intra prediction and constrained depth modelling mode provides very efficient prediction, resulting in a highly peaked residue distribution centered at zero. For this reason, PDC does not use the DCT, but an alternative approach which often assumes null residue and uses linear modelling in the other cases. The simplicity of the proposed approach is also advantageous in terms of computational complexity. Figure 6 illustrates the schematic of the proposed residue coding method. Four approximation models are available: constant, horizontal linear and vertical linear, as well as a special case of null residue. Depending on the chosen prediction mode, which is known in both the encoder and decoder, one of the residue approximation models should be transmitted. However, for a more efficient rate-distortion coding, PDC allows to bypass residue approximation, through the use of a binary flag. When the intensity range of the input depth map is quantised, the DLT algorithm is used.

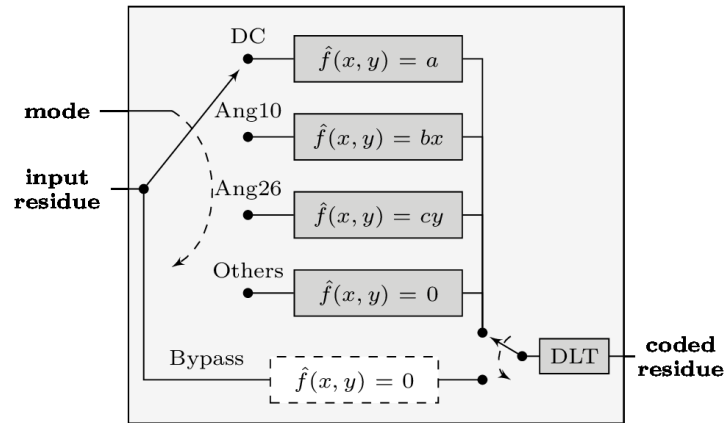


Figure 5: Detailed schematic of the PDC residue coding method.

### 3.5 Entropy Coding

The encoded bitstream contains the flags used to signal the block partition, the DLT information and the symbols produced by the encoder blocks: directional intra prediction, constrained depth modelling mode and residue coding. For entropy encoding, PDC employs the context adaptive binary arithmetic coding (CAAC) algorithm, based on the implementation of [5]. A different context model, which depends on the block size, is used for most of the transmitted symbols. In order to guarantee that PDC can independently decode each frame, the arithmetic encoder probability models are reset with uniform distribution for each frame.

## 4 Experimental Results

Simulations were run under the three-view configuration for the multiview video coding with depth data scenario, as proposed in common test conditions document for 3D video core experiments [6]. 3D-HEVC reference software HTM-8.2 was used for comparison purposes [7]. Since PDC algorithm is designed for intra coding, only spatial correlations are exploited. For a fair comparison with 3D-HEVC, all-intra configuration was used, without View Synthesis Optimisation (VSO) and the depth modelling modes that use inter component prediction of edges were disabled. PDC does not control the desired bitrate by the quantisation step size, but by the Lagrangian multiplier Lambda used in the encoder rate-distortion control. The following values have been used: 1200, 500, 250 and 75. Those lambdas allow a bitrate, which approximately corresponds to that generated by 3D-HEVC using the selected QPs.

The recommended depth map evaluation methodology by ISO/IEC and ITU-T JCT-3V group was used. It consists in assessing the quality of the generated virtual views, based on the decoded depth data and the original texture views versus exactly the same generated virtual views based on original uncompressed depth and original texture views. For evaluation purposes, the quality of six intermediate views placed between the positions of the encoded depth maps has been measured by luminance PSNR. For the purpose of view synthesis, state-of-the-art view synthesis software for linear camera arrangement implemented in HTM software has been used [7].

The experimental results, presented in Table 3, show the PSNR of each virtual view as well as the average PSNR for all views (avg-vv) for both PDC and 3D-HEVC algorithm. The sum of the bitrate (in kbits per second) used to encode the three depth maps and the average PSNR results of the virtual views were used to compute the Bjontegaard Delta Bitrate [8] (BD-BR) results shown in the last column of Table 3. These results clearly show the advantage of the proposed approach over the state-of-the-art 3D-HEVC standard. Note that PDC performance gains relative to 3D-HEVC are not constant, varying for different sequences. This is expected, since depth maps present distinct features that are differently exploited by PDC and 3D-HEVC algorithms.

For a valid evaluation of encoding performance, the tests were performed under similar conditions, using one core per running process, without other tasks causing additional load. The average number of seconds used to encode each depth map frame is shown in Table 4, for each rate point for each recommended test sequence using PDC and 3D-HEVC algorithms. PDC encoding times present an average reduction of 25% in computational complexity over 3D-HEVC standard, for depth map coding only.



Table 3: Rate-distortion performance of virtual views using depth maps encoded by PDC and 3D-HEVC algorithms.

Seq.	PDC									3D-HEVC							BD-rate	
	All views			PSNR of virtual views (vv)						All views		PSNR of virtual views (vv)						
	RP	Rate	PSNR	vv1	vv2	vv3	vv4	vv5	vv6	Rate	PSNR	vv1	vv2	vv3	vv4	vv5		vv6
Kendo	p4	456,44	40,73	43,87	41,84	41,72	40,08	38,35	38,53	474,11	40,78	43,97	41,86	41,88	40,01	38,20	38,78	2,85%
	p3	683,47	41,88	45,20	43,26	42,98	41,04	39,25	39,53	653,84	41,69	44,97	42,90	42,94	40,78	38,96	39,62	
	p2	940,28	42,95	46,32	44,43	44,35	41,89	40,15	40,54	888,25	42,67	45,94	43,93	44,05	41,53	39,86	40,70	
	p1	1609,54	45,10	48,54	46,63	46,87	43,65	42,07	42,84	1485,85	44,49	47,69	45,87	46,08	43,03	41,48	42,81	
U. Dancer	p4	393,16	37,60	37,75	37,12	37,96	37,73	37,10	37,92	426,74	37,31	37,85	36,56	37,54	37,88	36,54	37,47	1,69%
	p3	541,14	38,80	38,72	38,47	39,39	38,58	38,35	39,29	555,15	38,48	38,90	37,96	38,71	38,92	37,85	38,55	
	p2	697,54	39,90	39,57	39,69	40,53	39,55	39,59	40,46	704,69	39,95	40,05	39,50	40,25	40,15	39,51	40,21	
	p1	1077,78	41,96	41,42	41,92	42,82	41,36	41,73	42,49	1003,55	42,12	41,62	41,84	42,80	41,87	41,84	42,76	
GT Fly	p4	543,66	41,40	41,87	40,35	42,09	42,05	40,31	41,73	605,48	41,33	41,81	40,24	42,03	41,98	40,20	41,71	10,81%
	p3	843,53	42,64	43,07	41,57	43,37	43,30	41,56	42,96	840,43	42,32	42,77	41,24	43,02	42,98	41,21	42,70	
	p2	1210,91	43,84	44,27	42,78	44,59	44,51	42,75	44,13	1195,86	43,47	43,92	42,41	44,21	44,14	42,34	43,82	
	p1	2211,44	46,19	46,56	45,15	46,99	46,90	45,11	46,41	2108,34	45,52	45,89	44,46	46,31	46,23	44,42	45,79	
Balloons	p4	517,45	44,29	44,39	43,17	45,20	45,04	43,31	44,62	539,54	44,40	44,52	43,35	45,26	45,15	43,41	44,68	0,93%
	p3	794,19	45,58	45,63	44,47	46,49	46,27	44,68	45,96	755,96	45,46	45,56	44,41	46,36	46,16	44,53	45,77	
	p2	1121,34	46,71	46,74	45,64	47,64	47,40	45,83	47,03	1041,51	46,45	46,50	45,39	47,33	47,17	45,55	46,77	
	p1	1989,73	48,92	48,82	47,92	49,92	49,53	48,09	49,24	1783,67	48,24	48,21	47,26	49,11	48,90	47,40	48,54	
Newspaper_CC	p4	666,30	39,20	38,72	37,82	39,86	40,43	38,35	40,03	714,13	39,38	38,93	38,04	40,09	40,58	38,45	40,20	-1,26%
	p3	1067,29	40,43	39,78	39,01	41,08	41,70	39,64	41,34	1013,98	40,34	39,72	38,91	40,90	41,64	39,58	41,29	
	p2	1553,10	41,43	40,73	40,06	42,22	42,59	40,61	42,38	1406,82	41,21	40,57	39,83	41,88	42,40	40,48	42,12	
	p1	2805,18	43,25	42,32	41,95	44,13	44,38	42,44	44,27	2416,70	42,74	41,95	41,45	43,48	43,96	42,00	43,62	
P. Street	p4	443,89	43,23	44,32	42,38	44,10	43,63	41,55	43,41	454,99	43,06	44,14	42,16	43,99	43,41	41,39	43,26	1,46%
	p3	678,13	44,33	45,43	43,53	45,18	44,70	42,68	44,50	652,06	44,19	45,21	43,30	45,06	44,59	42,54	44,42	
	p2	986,16	45,16	46,20	44,34	46,09	45,56	43,50	45,25	940,07	45,05	46,07	44,21	45,96	45,43	43,38	45,25	
	p1	1979,48	46,64	47,59	45,93	47,63	47,02	44,92	46,73	1763,47	46,41	47,39	45,70	47,35	46,75	44,72	46,54	
P. Hall2	p4	204,67	46,27	46,87	44,76	46,44	47,37	45,29	46,86	204,33	46,24	46,87	44,88	46,38	47,22	45,32	46,79	5,69%
	p3	273,79	47,85	48,49	46,41	47,91	49,04	46,97	48,29	262,88	47,44	48,00	46,08	47,50	48,45	46,61	47,97	
	p2	354,10	49,12	49,86	47,70	49,12	50,37	48,26	49,43	339,34	48,64	49,08	47,26	48,72	49,71	47,83	49,21	
	p1	571,05	51,48	52,20	49,98	51,40	52,88	50,61	51,79	541,03	50,66	51,04	49,18	50,60	51,86	50,01	51,26	
Shark	p4	1135,87	41,71	42,01	40,86	42,21	42,15	40,92	42,10	1253,88	41,72	42,05	40,79	42,21	42,23	40,87	42,16	8,10%
	p3	1893,69	43,30	43,56	42,44	43,83	43,76	42,51	43,71	1849,10	42,96	43,30	42,04	43,46	43,48	42,12	43,39	
	p2	2704,78	44,64	44,87	43,75	45,18	45,11	43,86	45,07	2652,30	44,29	44,57	43,33	44,80	44,83	43,46	44,73	
	p1	4728,10	47,09	47,24	46,16	47,72	47,53	46,28	47,59	4575,61	46,50	46,78	45,54	47,01	47,07	45,67	46,93	

Table 4: Encoding time results (in seconds per frame) for each rate-distortion point and recommended depth map test sequences using PDC and 3D-HEVC algorithms.

Test sequences	PDC (seconds per frame)					3D-HEVC, only depth (secs per frame)					Ratio				
	p4	p3	p2	p1	Avg	p4	p3	p2	p1	Avg	p4	p3	p2	p1	Avg
Kendo	5,24	6,17	7,07	8,03	<b>6,63</b>	7,06	8,04	7,22	7,66	<b>7,49</b>	0,74	0,77	0,98	1,05	<b>0,88</b>
Dancer	8,40	9,82	11,49	13,49	<b>10,80</b>	18,26	19,74	20,33	23,09	<b>20,36</b>	0,46	0,50	0,57	0,58	<b>0,53</b>
GT Fly	11,14	12,97	14,70	18,06	<b>14,21</b>	19,28	21,33	22,29	24,72	<b>21,90</b>	0,58	0,61	0,66	0,73	<b>0,65</b>
Balloons	5,89	7,02	7,86	8,70	<b>7,37</b>	6,58	6,89	7,64	7,57	<b>7,17</b>	0,89	1,02	1,03	1,15	<b>1,03</b>
Newspaper	7,87	9,12	10,23	11,83	<b>9,77</b>	8,82	8,43	8,92	9,38	<b>8,89</b>	0,89	1,08	1,15	1,26	<b>1,10</b>
Poznan Street	9,17	11,16	13,89	18,88	<b>13,28</b>	17,55	18,84	22,58	23,44	<b>20,60</b>	0,52	0,59	0,62	0,81	<b>0,64</b>
Poznan Hall2	5,16	6,43	7,41	9,46	<b>7,11</b>	17,58	18,22	18,10	18,80	<b>18,17</b>	0,29	0,35	0,41	0,50	<b>0,39</b>
<b>Average</b>	<b>7,55</b>	<b>8,96</b>	<b>10,38</b>	<b>12,63</b>	<b>9,88</b>	<b>13,59</b>	<b>14,50</b>	<b>15,30</b>	<b>16,38</b>	<b>14,94</b>	<b>0,63</b>	<b>0,70</b>	<b>0,77</b>	<b>0,87</b>	<b>0,75</b>

## 5 Conclusions

PDC is presented as an alternative algorithm to the 3D-HEVC for depth map coding, worth further investigation. Experimental results demonstrate the better performance of PDC compared with the current state-of-the-art depth coding techniques used in 3D-HEVC standard in terms of its rate-distortion performance for the synthesised views, as well as a decrease of about 25% in the computational complexity. As future work, PDC algorithm could be extended to include inter prediction techniques for efficient coding of temporal and inter-view redundancies, and to use the VSO method as a distortion control method.

## 6 References

- [1] G. Tech, K. Wegner, Y. Chen, S. Yea, „3D-HEVC Draft Text 4”, Joint Collaborative Team on 3D Video Coding Extension Development of ITU-T SG 16 WP 3 and ISO/IEC JTC 1/SC 29/WG 11 Doc. JTC3V-H1001, 8th Meeting: Valencia, ES, 29 March – 4 April 2014
- [2] Y. Morvan, P. H. N. de With, D. Farin, “Platelet-based coding of depth maps for the transmission of multiview images”, Proceedings of SPIE: Stereoscopic Displays and Applications, Vol. 6055 (2006)
- [3] L. F. R. Lucas, N. M. M. Rodrigues, C. L. Pagliari, E. A. B. da Silva, and S. M. M. de Faria, “Predictive depth map coding for efficient virtual view synthesis”, IEEE Int. Conf. on Image Proc., September 2013
- [4] G.J. Sullivan, J.-R. Ohm, W.-J. Han, T. Wiegand, “Overview of the High Efficiency Video Coding (HEVC) Standard”, IEEE Transactions on Circuits and Systems for Video Technology, 2012, 22, (12), pp. 1649-1668, doi: 10.1109/TCSVT.2012.2221191
- [5] D. Marpe, H. Schwarz, and T. Wiegand, “Context-based adaptive binary arithmetic coding in the H.264/AVC video compression standard,” Circuits and Systems for Video Technology, IEEE Transactions on, vol. 13, no. 7, pp. 620–636, 2003
- [6] "Common Test Conditions of 3DV Core Experiments" Joint Collaborative Team on 3D Video Coding Extension Development of ITU-T SG 16 WP 3 and ISO/IEC JTC 1/SC 29/WG 11, Document: JCT3V-G1100, 7th Meeting: San José, USA, 11–17 Jan. 2014
- [7] L. Zhang, G. Tech, K. Wegner, S. Yea, „Test Model 8 of 3D-HEVC and MV-HEVC”, Joint Collaborative Team on 3D Video Coding Extension Development of ITU-T SG 16 WP 3 and ISO/IEC JTC 1/SC 29/WG 11 Doc. JTC3V-H1005, 8th Meeting: Valencia, ES, 29 March – 4 April 2014

- [8] G. Bjøntegaard, "Calculation of average PSNR differences between RD-curves," ITU-T SG 16 Q.6 VCEG, Doc. VCEG-M33, 2001